International Journal of Bio-Science and Bio-Technology
Vol.7, No.3 (2015), pp.111-120
http://dx.doi.org/10.14257/ijbsbt.2015.7.3.11

Camera Calibration Using Direct Mapping and Adaptive Metaheuristics

Jaroslav Moravec[1] and Miloslav Hub[2]

[1,2]Faculty of Economics and Administration, University of Pardubice, Pardubice, Czech Republic
j.moravec.email@seznam.cz, http://handwork.4fan.cz/,
miloslav.hub@upce.cz, http://hub.upce.cz/

Abstract

Every optical system is influenced with a set of aberrations. Some of them are corrected by the manufacturer of the optical system, other aberrations must be corrected additionally e.g. using methods of digital image correction. The presented paper describes a method which enables correction of a barrel or pillow distortion of an image of small range using the direct-mapping technique. The proposed method uses an algorithm of adaptive metaheuristics marked as jDE and a polynomial representation of the image distortion. The advantage of connecting direct mapping technique and adaptive metaheuristics is primarily high speed of finding basic coefficients of the correction polynomial; in our case it is polynomial of degree up to 7 and with a selectable combination of the used polynomial degrees. The disadvantage of the direct-mapping method is the necessity of reconstruction of the missing pixels in the final image, which is here solved very effectively by using optimizer jDE again. Using the proposed method it is possible to obtain high quality image free of barrel or pillow distortion. If the focus length of the used optical system is constant, values of the correction coefficients and positions of individual recovered pixels stay invariable as well

Keywords: *Distortion removing, Evolutionary computation, Camera calibration, Adaptive metaheuristics*

1. Introduction

Unwanted aberrations of the optical systems [9] can be corrected in many different ways. Most of them are corrected at design and manufacturing of the optical system. Other aberrations such as distortion can be corrected at taking the picture if digital processing technology is used. The correction process is done either by the processor according to an algorithm prepared before or by a programmable logic array *e.g.*, for studio recording devices which can be significantly faster, however, less flexible.

Basic methodology of image distortion correction both for centric or non-centric aberration was described earlier in 1919 by Prof. A.E. Conrady [1]. In later years proposed methods were extended by many other authors *e.g.*, [2] and [3]. As a referential in the area is very often considered article of Dunkan C. Brown [4] which is based on so called polynomial-radial model and which is used up to these days. Besides the methods which are based on polynomial model there are methods based on non-polynomial model *e.g.*, [7]. Their advantage is faster computation; hence, they can be used for camera objectives with variable focal length without hardware acceleration. The disadvantage is smaller universality and to some extent some bonding to concrete type of optical system resp. concrete distortion magnitude *e.g.*, for Fish-Eye camera objectives. The methods used for aberration correction are further divided to so called Back-mapping [4, 5] and Direct-mapping [8] methods. Computation speed, if correction coefficients are known, is identical for both the systems. The advantage of the first method is that in final image there are no blank spaces – missing pixels as a consequence of imperfect mapping; this rule is valid at least for small distortion of an image. The second method provides as good image correction as the first method, but the correction process is burdened with many inaccuracies at mapping and there is a large amount of information missing in the final image – missing pixels which are not correctly coloured. Colours of the missing pixels can be obtained either as an average colour from neighbouring pixels or for the small degree of the correction polynomial (max. degree 3) can be computed using Cardan polynomials – see [8]. If correction polynomial has higher degree (higher that 5), there is no simple way which would be capable of finding an accurate correspondence between pixels in distorted image and in resulting corrected image. The only possible way is to use methods of numerical mathematics.

A part of the proposed method for image distortion removing is also algorithm from area of evolutionary computation called jDE by its authors – see [5]. It is an advanced evolutionary algorithm derived from Differential Evolution optimizer [10]. However, jDE is a very young and powerful stochastic optimizer – metaheuristic, which was presented in 2006. jDE is used for both finding correction coefficients and also for finding of the colour of the missing pixels in final image. The method for ascertaining correct colouration of the missing pixels uses technique of inverse engineering – seeking for the correct position of the pixel in the distorted image using known coefficients of correction polynomial and then the colour of the pixel is copied back to the undistorted image.

The proposed method for camera calibration will be hereafter marked as DMAM (**D**irect **M**apping calibration algorithm using **A**daptive **M**etaheuristics).

2. Experimental Section

At assembling of the algorithm which is presented in here for correction of the distortion aberration following sources were used: polynomial algorithm was obtained from [1, 4] and also from [9], consideration of possibility to use direct-mapping method for given purposes is presented in *e.g.*, [6] and also in [8], where also evolutionary algorithm SGA is simultaneously used and finally there was used advanced evolutionary optimizer jDE assumed from [5, 10] - see **Algorithm** 4. Brown [3, 4] used in his work for distortion aberration correction multinomial $\mathcal{F}_{odd}$ which is build-up of odd power:

$$\mathcal{F}_{odd}(r_d) \equiv r_u = \sum_{n=2m+1, m\in\mathbb{N}^0}^{N_{odd}} c_n r_d^n = c_1 r_d^1 + c_3 r_d^3 + c_4 r_d^5 \dots c_{N_{odd}} r_d^{N_{odd}} \quad (1)$$

where r_d is distance of the pixel from centre of the distorted image $\boldsymbol{I_D}$and r_u is distance of the pixel from centre of the undistorted image $\boldsymbol{I_U}$. Brown's algorithm has very high approximation accuracy approx. 97%. Of course, to correct the image such a polynomial $\mathcal{F}$ can be used which uses both odd and even powers and final result is identical or better – see [3,4]. This approach is used in algorithm DMAM. Polynomial $\mathcal{F}$ is then defined as:

$$\mathcal{F}(r_d) \equiv r_u = \sum_{n=1}^{N} c_n r_d^n = c_1 r_d^1 + c_2 r_d^2 + c_3 r_d^3 + c_4 r_d^4 \dots c_N r_d^N \quad (2)$$

The method DMAM is destined for barrel or pillow aberration correction of an image obtained from a biometric scanner – see Figure 1B, C, which is scanned by a camera with a small focal length. However, it is possible to use this method to correct barrel or pillow distortion for any image. The biometrical scanner uses classic digital compact camera CanonPowerShotS60, which is strongly fixed at the part of the scanned and camera can be adjusted in axes XYZ and in plane XY – see Figure 1C. First, colour (RGB) calibration image $\boldsymbol{I_D'}'$ is obtained**,** which is transformed to B&W image $\boldsymbol{I_D}$of identical resolution –

see Figure 2B**.** The image $\boldsymbol{I_D}$ contains a set of calibration marks $\boldsymbol{M}_C$, every of them in size of 20x20 pixels. Using knowledge of geometrical centre of set of marks and mutual distances of single marks on original calibration drawing, referential matrix $\boldsymbol{M}_R$ is designed manually – it defines ideal positions of the calibration marks in the image without distortion. The aim of the algorithm DMAM is to find such values of the coefficients $c_i, i \in \langle 1, N \rangle$ resp. vector $\boldsymbol{C_f}$ of the multinomial $\mathcal{F}$, which enable correct transformation of the image $\boldsymbol{I_D}$to image$\boldsymbol{I_U}$**.** The result of transformation is then given by matrix $\boldsymbol{M}_F$ which represents the best estimation of the coefficients c_i of the vector $\boldsymbol{C_f}$. Matrixes $\boldsymbol{M}_C, \boldsymbol{M}_R$ and $\boldsymbol{M}_F$ are defined as:

$$\boldsymbol{M_C} = \begin{bmatrix} (\ddot{x},\ddot{y})_{0,0} & \dots & (\ddot{x},\ddot{y})_{0,\mathrm{j}} \\ \dots & \dots & \dots \\ (\ddot{x},\ddot{y})_{\mathrm{i},0} & \dots & (\ddot{x},\ddot{y})_{\mathrm{i,j}} \end{bmatrix}, \boldsymbol{M_F} = \begin{bmatrix} (\hat{x},\hat{y})_{0,0} & \dots & (\hat{x},\hat{y})_{0,\mathrm{j}} \\ \dots & \dots & \dots \\ (\hat{x},\hat{y})_{\mathrm{i},0} & \dots & (\hat{x},\hat{y})_{\mathrm{i,j}} \end{bmatrix}, \boldsymbol{M_R} = \begin{bmatrix} (x,y)_{0,0} & \dots & (x,y)_{0,\mathrm{j}} \\ \dots & \dots & \dots \\ (x,y)_{\mathrm{i},0} & \dots & (x,y)_{\mathrm{i,j}} \end{bmatrix}, \quad (3)$$

$$\hat{x},\hat{y} \in \mathcal{H}_U;\ x,y \in \mathcal{H}_U;\ \ddot{x},\ddot{y} \in \mathcal{H}_D$$

$$\mathrm{i} \in \langle 0, I_w - 1\rangle,\ \mathrm{j} \in \langle 0, I_h - 1\rangle,\ x,y \in \mathbb{N}^0;\ \hat{x},\hat{y} \in \mathbb{R}^+;\ \ddot{x},\ddot{y} \in \mathbb{R}^+,$$

$\mathcal{H}_U, \mathcal{H}_D$-space of coordinates in undistorted and distorted image.

(**A**) DMAM algorithm Schematic diagram	(**B**) Biometric scanner	(**C**) Biometric scanner functional scheme

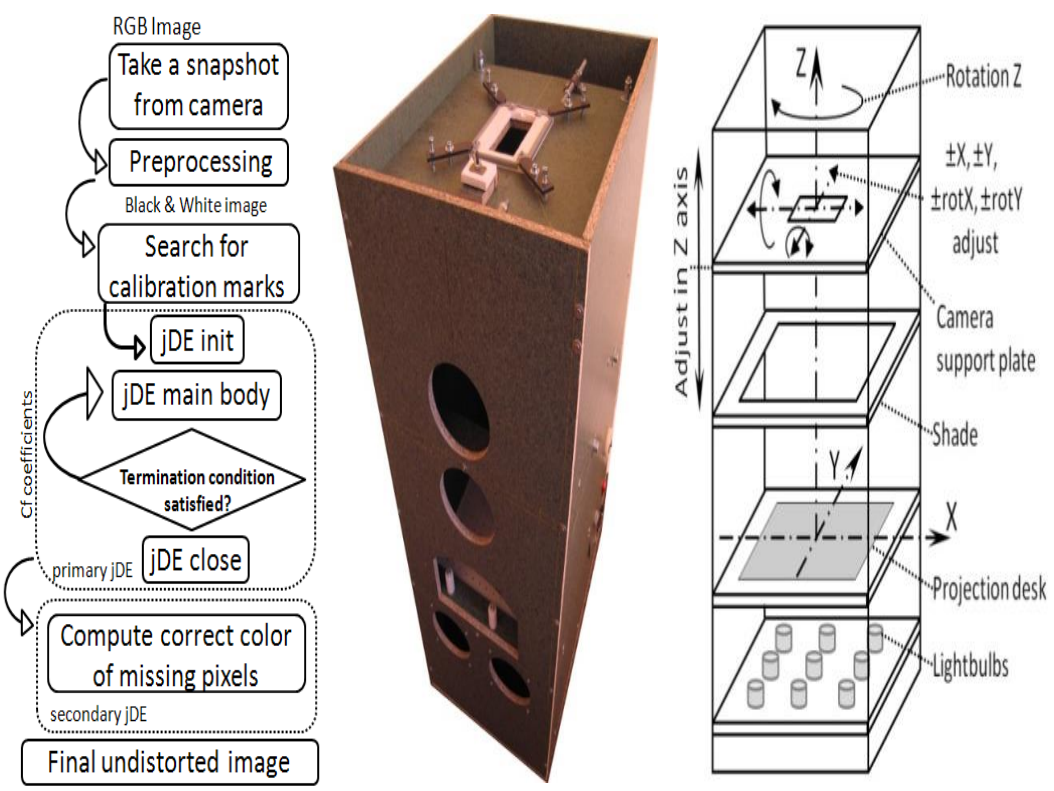

Figure 1. Used Biometric Scanner (B) and its Functional Scheme (C) and Schematic Chart of Proposed DMAM Algorithm (A)

and values $(\ddot{x}, \ddot{y})$ represents positions of the centre of masses of the calibration marks, $(\hat{x}, \hat{y})$ are the final estimation positions after transformation using multinomial $\mathcal{F}$. For primary location of the marks $\boldsymbol{M_C}$ in the image $\boldsymbol{I_D}$an algorithm is used, which cyclically seeks expected number of black pixels (*e.g.*, 350) in squared area of size 20x20 pixels. A squared area moved across the whole area of image $\boldsymbol{I_D}$ step by step, pixel by pixel. The proposed algorithm DMAM is depicted in **Algorithm 1,2,3. A** schematic chart of DMAM is displayed in Figure 1A. First, using the jDE optimizer, marked here as 'primary jDE' correct coefficients c_i of the vector $\boldsymbol{C_f}$ are found.

Algorithm 1, Proposed DMAM algorithm

Input:$\boldsymbol{I_D}, \boldsymbol{M_R}, T_2, T_1$, jDE parameters, A_S mask ;
Output: $\boldsymbol{C_f}, \boldsymbol{I_U}$

Get $\boldsymbol{I_D''}$ from camera
$\boldsymbol{I_D''}$ to grayscale + thresholding; $\boldsymbol{I_D''} \rightarrow \boldsymbol{I_D}$
Seek for $\boldsymbol{M_C}$in$\boldsymbol{I_D}$
Init primary jDE; Create $\boldsymbol{P_{op}}^{\boldsymbol{jDE}}$
Evaluate $\boldsymbol{P_{op}}^{\boldsymbol{jDE}}$; sort$\boldsymbol{P_{op}}^{\boldsymbol{jDE}}$; find $\boldsymbol{X_{best}}^{\boldsymbol{jDE}}$
while (T_1 is not satisfied)
for i=0; i <N^{jDE}; i=i+1
$\boldsymbol{X_i}^{\boldsymbol{jDE}}.F_{old} = \boldsymbol{X_i}^{\boldsymbol{jDE}}.F$; $\boldsymbol{X_i}^{\boldsymbol{jDE}}.P_{cr-old} = \boldsymbol{X_S}^{\boldsymbol{jDE}}.P_{cr}$
if$rand(0,1) < \boldsymbol{\tau_1}$: $\boldsymbol{X_i}^{\boldsymbol{jDE}}.F = F_l + F_u * rand(0,1)$
if$rand(0,1) < \boldsymbol{\tau_2}$: $\boldsymbol{X_i}^{\boldsymbol{jDE}}.P_{cr} = rand(0,1)$
  Select $\{\boldsymbol{X_{r1}}, \boldsymbol{X_{r2}}, \dots, \boldsymbol{X_{rk}}\}, rj \neq i, \boldsymbol{X_{rj}} \in \boldsymbol{P_{op}}^{\boldsymbol{jDE}}$
  Compute $\boldsymbol{X_t}$ using $\overline{\boldsymbol{V_p}}, \boldsymbol{X_i}^{\boldsymbol{jDE}}, \boldsymbol{X_{rj}}, \boldsymbol{X_{best}}^{\boldsymbol{jDE}}$
  $R_1 = fitness_1(\boldsymbol{X_i}^{\boldsymbol{jDE}}.x_1, \boldsymbol{X_i}^{\boldsymbol{jDE}}.x_2)$
$R_2 = fitness_1(\boldsymbol{X_t}.x_1, \boldsymbol{X_t}.x_2)$ - trial vect.
if$R_1 < R_2$:
$\boldsymbol{X_i}^{\boldsymbol{jDE}}.F = F_{old}$; $\boldsymbol{X_i}^{\boldsymbol{jDE}}.P_{cr} = P_{cr-old}$
if$R_1 \geq R_2$:
$\forall j, j \in \langle 0, D_{im}) : \boldsymbol{X_i}^{\boldsymbol{jDE}}.x_j = \boldsymbol{X_t}.x_j$
endfor
Sort$\boldsymbol{P_{op}}^{\boldsymbol{jDE}}$; find $\boldsymbol{X_{best}}^{\boldsymbol{jDE}}$ in $\boldsymbol{P_{op}}^{\boldsymbol{jDE}}$
endwhile
Delete $\boldsymbol{P_{op}}^{\boldsymbol{jDE}}$; $\boldsymbol{C_f} = \boldsymbol{X_{best}}^{\boldsymbol{jDE}}.\boldsymbol{C_f}$- final coefs.
Use $\boldsymbol{C_f}$andcompute $\boldsymbol{I_U}$; close primary jDE
for u=0; u <$\boldsymbol{I_U}\_width$; u=u+1
for v=0; v <$\boldsymbol{I_U}\_height$; v=v+1
if$\boldsymbol{I_U}[u,v]$is already coloured: continue;
$P_W.x = u$; $P_W.y = v$ - target pixel position
  Init secondary jDE; Create $\boldsymbol{P_{op}}^{\boldsymbol{jDE}}$
  Evaluate $\boldsymbol{P_{op}}^{\boldsymbol{jDE}}$; sort$\boldsymbol{P_{op}}^{\boldsymbol{jDE}}$; find $\boldsymbol{X_{best}}^{\boldsymbol{jDE}}$
while (T_2 is not satisfied)
for i=0; i <N^{jDE}; i=i+1
$\boldsymbol{X_i}^{\boldsymbol{jDE}}.F_{old} = \boldsymbol{X_i}^{\boldsymbol{jDE}}.F$; $\boldsymbol{X_i}^{\boldsymbol{jDE}}.P_{cr-old} = \boldsymbol{X_S}^{\boldsymbol{jDE}}.P_{cr}$
if$rand(0,1) < \boldsymbol{\tau_1}$ **then**
  $\boldsymbol{X_i}^{\boldsymbol{jDE}}.F = F_l + F_u * rand(0,1)$
if$rand(0,1) < \boldsymbol{\tau_2}$:
  $\boldsymbol{X_i}^{\boldsymbol{jDE}}.P_{cr} = rand(0,1)$
  Select $\{\boldsymbol{X_{r1}}, \boldsymbol{X_{r2}}, \dots, \boldsymbol{X_{rk}}\}, rj \neq i, \boldsymbol{X_{rj}} \in \boldsymbol{P_{op}}^{\boldsymbol{jDE}}$
  Compute $\boldsymbol{X_t}$ using $\overline{\boldsymbol{V_p}}, \boldsymbol{X_i}^{\boldsymbol{jDE}}, \boldsymbol{X_{rj}}, \boldsymbol{X_{best}}^{\boldsymbol{jDE}}$
  $R_1 = fitness_2(\boldsymbol{X_i}^{\boldsymbol{jDE}}.x_1, \boldsymbol{X_i}^{\boldsymbol{jDE}}.x_2)$
$R_2 = fitness_2(\boldsymbol{X_t}.x_1, \boldsymbol{X_t}.x_2)$ - trial vect.
if$R_1 \leq R_2$:
$\boldsymbol{X_i}^{\boldsymbol{jDE}}.F = F_{old}$; $\boldsymbol{X_i}^{\boldsymbol{jDE}}.P_{cr} = P_{cr-old}$
if$R_1 > R_2$:
$\forall j, j \in \langle 0, D_{im}) : \boldsymbol{X_i}^{\boldsymbol{jDE}}.x_j = \boldsymbol{X_t}.x_j$
endfor
Sort$\boldsymbol{P_{op}}^{\boldsymbol{jDE}}$; find $\boldsymbol{X_{best}}^{\boldsymbol{jDE}}$ in $\boldsymbol{P_{op}}^{\boldsymbol{jDE}}$
endwhile
  $\boldsymbol{I_U}[u,v] = \boldsymbol{I_D}[\boldsymbol{X_{best}}^{\boldsymbol{jDE}}.x_1, \boldsymbol{X_{best}}^{\boldsymbol{jDE}}.x_2]$
  Delete $\boldsymbol{P_{op}}^{\boldsymbol{jDE}}$
endfor
endfor

Algorithm 2, $fitness_1$ computation

Input: $\boldsymbol{M_C}, \boldsymbol{M_R}, \widehat{\boldsymbol{C_f}} \equiv \boldsymbol{X_i}^{\boldsymbol{jDE}}.\boldsymbol{C_f}$or $\boldsymbol{X_t}.\boldsymbol{C_f}$

$fitness_1 = 0$; $d = max(I_w, I_h)$
for i=0; i <M_{CX}; i=i+1
for j=0; j <M_{CY}; j=j+1
$center_X = 0.5 \times (I_w - 1)$; $center_Y = 0.5 \times (I_h - 1)$;
$\Delta_X = \frac{(M_C[i,j].x - center_X)}{d}$; $\Delta_Y = \frac{(M_C[i,j].y - center_Y)}{d}$
$R_d = \sqrt{\Delta_X{}^2 + \Delta_Y{}^2}$; $f = \frac{R_d}{R_s}$;
$R_s = \sum_{i=1}^{i=Dim^{primary-jDE}} [\widehat{c_i} \times (R_d)^i]$;
$X_S = center_X + (f \times \Delta_X \times d)$;
$Y_S = center_Y + (f \times \Delta_Y \times d)$
$fitness_1 =$
$= fitness_1 + \sqrt{(X_S - M_R[i,j].x)^2 + (Y_S - M_R[i,j].y)^2}$
endfor
endfor

Algorithm 3, $fitness_2$ computation

Input:$I_w, I_h, \boldsymbol{C_f}, P_W, t_R \equiv \boldsymbol{X_i}^{\boldsymbol{jDE}}$ or$\boldsymbol{X_t}(\boldsymbol{x}, \boldsymbol{y})$

$center_X = 0.5 \times (I_w - 1)$; $center_Y = 0.5 \times (I_h - 1)$;
$d = max(I_w, I_h)$;
$\Delta_X = \frac{(t_R.x - center_X)}{d}$; $\Delta_Y = \frac{(t_R.y - center_Y)}{d}$
$R_d = \sqrt{\Delta_X{}^2 + \Delta_Y{}^2}$; $f = \frac{R_d}{R_s}$
$R_s = \sum_{i=1}^{i=Dim^{secondary-jDE}} [c_i \times (R_d)^i]$;
$X_S = center_X + (f \times \Delta_X \times d)$;
$Y_S = center_Y + (f \times \Delta_Y \times d)$
$fitness_2 = \sqrt{(X_S - P_W.x)^2 + (Y_S - P_W.y)^2}$

Algorithm 4, Original jDE optimizer algorithm – see [5]

Select $N, F_l, F_u, \tau_1, \tau_2, \overline{\boldsymbol{V_p}}, T$; Given D_{im}, D_{om}
Create $\boldsymbol{P_{op}}^{\boldsymbol{jDE}} = (\boldsymbol{X_1}, \dots, \boldsymbol{X_N}), \boldsymbol{X_i}^{\boldsymbol{jDE}} = [x_j | \mathrm{j} \in \langle 0, \mathrm{D_{im}}), F, P_{cr}]$
for i = 0; i <N; i=i+1
for j = 0; j <D_{im}; j=j+1
  Init $\boldsymbol{X_i}^{\boldsymbol{jDE}}.x_j$ randomly in D_{om}
  $\boldsymbol{X_i}^{\boldsymbol{jDE}}.F = rand$; $\boldsymbol{X_i}^{\boldsymbol{jDE}}.P_{cr} = rand$
endfor
endfor
Evaluate $\boldsymbol{P_{op}}^{\boldsymbol{jDE}}$; find the best ind. $\boldsymbol{X_{best}}^{\boldsymbol{jDE}}$
while (T is not satisfied)
for i = 0; i < N; i=i+1
$F_{old} = \boldsymbol{X_i}^{\boldsymbol{jDE}}.F$; $P_{cr-old} = \boldsymbol{X_i}^{\boldsymbol{jDE}}.P_{cr}$
Compute new$\boldsymbol{X_i}^{\boldsymbol{jDE}}.F$, $\boldsymbol{X_i}^{\boldsymbol{jDE}}.P_{cr}$
  Select randomly $\{\boldsymbol{X_{r1}}, \boldsymbol{X_{r2}}, \dots, \boldsymbol{X_{rk}}\}, rj \neq i, \boldsymbol{X_{rj}} \in \boldsymbol{P_{op}}$
  Compute trial vector $\boldsymbol{X_t}$using$\overline{\boldsymbol{V_p}}, \boldsymbol{X_i}, \boldsymbol{X_{rj}}, \boldsymbol{X_{best}}$
if$fitness(\boldsymbol{X_i}^{\boldsymbol{jDE}})$ is better than$fitness(\boldsymbol{X_t})$
$\boldsymbol{X_i}^{\boldsymbol{jDE}}.F = F_{old}$; $\boldsymbol{X_i}^{\boldsymbol{jDE}}.P_{cr} = P_{cr-old}$
else
$\boldsymbol{X_i}^{\boldsymbol{jDE}}.x_j = \boldsymbol{X_t}.x_j | \mathrm{j} \in \langle 0, \mathrm{D_{im}})$;
endif
endfor
 Find best ind. $\boldsymbol{X_{best}}^{\boldsymbol{jDE}}in\boldsymbol{P_{op}}^{\boldsymbol{jDE}}$
endwhile
$\boldsymbol{X_{best}}^{\boldsymbol{jDE}}$ represents the best estimated solution

Key:$\boldsymbol{P_{op}}^{\boldsymbol{jDE}}$-population of individuals; N-the number of individuals, for the primary jDE optimizer $\boldsymbol{X_i}^{\boldsymbol{jDE}}(x_1, \dots, x_7) \in \mathbb{R}$, $D_{im} = 7$, $x_i$is usually in range $\langle -2.0, +2.0 \rangle$ and for the secondary jDE optimizer is $\boldsymbol{X_i}^{\boldsymbol{jDE}}(x_1, x_2) \in \boldsymbol{I_D}$, $D_{im} = 2$; $F, P_{cr}, \tau_1, \tau_2, F_l, F_u$-jDE working parameters; $\overline{\boldsymbol{V_p}}$-perturbation vector; D_{im}-number of dimensions of every individual; D_{om}-domain for every single D_{im}; T, T_1, T_2-termination conditions; $\boldsymbol{X_i}^{\boldsymbol{jDE}}$-chromosome of every individual or one possible solution of the given task; pays, that $\boldsymbol{X_{r1}} \neq \boldsymbol{X_{r2}} \neq \cdots \neq \boldsymbol{X_{rk}} \neq \boldsymbol{X_i}^{\boldsymbol{jDE}}$, the number of $\boldsymbol{X_{rk}}$ vectors is given by $\overline{\boldsymbol{V_p}}$;$\boldsymbol{X_t}$-trial vector or individual obtained using $\overline{\boldsymbol{V_p}}$; $\boldsymbol{X_{best}}^{\boldsymbol{jDE}}$-best individual in every generation; $\boldsymbol{I''_D}$-the RGB image from camera; $\boldsymbol{I_D}$-preprocessed distorted B&W image; $\boldsymbol{I_U}$-undistorted image; $P_W(x, y)$-auxiliary variable; $\boldsymbol{M_C}$-matrix of the calibration marks, poses of calibration marks is obtained from$\boldsymbol{I_D}$; $\boldsymbol{M_R}$-matrix of poses of the referential marks obtained by hand measurement; M_{CX}, M_{CY}-the sizes of the matrixes $\boldsymbol{M_C}$and$\boldsymbol{M_R}$, size of $\boldsymbol{M_C}$and$\boldsymbol{M_R}$is identical; I_w-image width; I_h-image height; $\boldsymbol{C_f}$ - vector of coefficients of the equalization multinomial; I_w, I_h-is usually counted from 0; the size of $\boldsymbol{I_U}$and $\boldsymbol{I_D}$ is identical; T_1 and T_2 are defined as fixed number of generations, usually $T_1 = 120, T_2 = 60$. So called 'dot-notation' is used in the algorithms if certain dimension or variable in the record is referenced, on the ground of algorithm development every individual is assumed as record: $\boldsymbol{X_i}^{\boldsymbol{primary-jDE}} = \{\boldsymbol{x}, fit, F, P_{cr}, F_{old}, P_{cr-old}\}$ where $\boldsymbol{x} = (x_1, \dots, x_7)$ and similarly for $\boldsymbol{X_i}^{\boldsymbol{secondary-jDE}}$where$\boldsymbol{x} = (x_1, x_2)$. $\widehat{\boldsymbol{C_f}}$-auxiliary variable.

The vector $\boldsymbol{C_f}$ is then installed into multinomial $\mathcal{F}$ and the image $\boldsymbol{I_D}$is transformed to image$\boldsymbol{I_U}$ **-** see **Algorithm 1**, r. 4-21. Because thedirect-mapping method is used [8], some pixels of image $\boldsymbol{I_U}$are not coloured – see Figure 3B. In the second part of the algorithm DMAM optimized jDE is used again; it seeks corresponding pixels in the image $\boldsymbol{I_D}$for single missing pixels of the image $\boldsymbol{I_U}$using vector $\boldsymbol{C_f}$ obtained by 'primary jDE' **-** see **Algorithm 1**, r. 22-45. The main advantage of the proposed algorithm is that the correction multinomial $\mathcal{F}$ can be of any degree and with any combination of degrees – powers. In experiments is used max. degree 7 (all 7 degrees). Figure 2 displays work results of the algorithm DMAM again with the use of all 7 degrees.

(A) Regular Undistorted Image	(B) Distorted Image Obtained from the Camera	(C) Corrected Image using DMAM

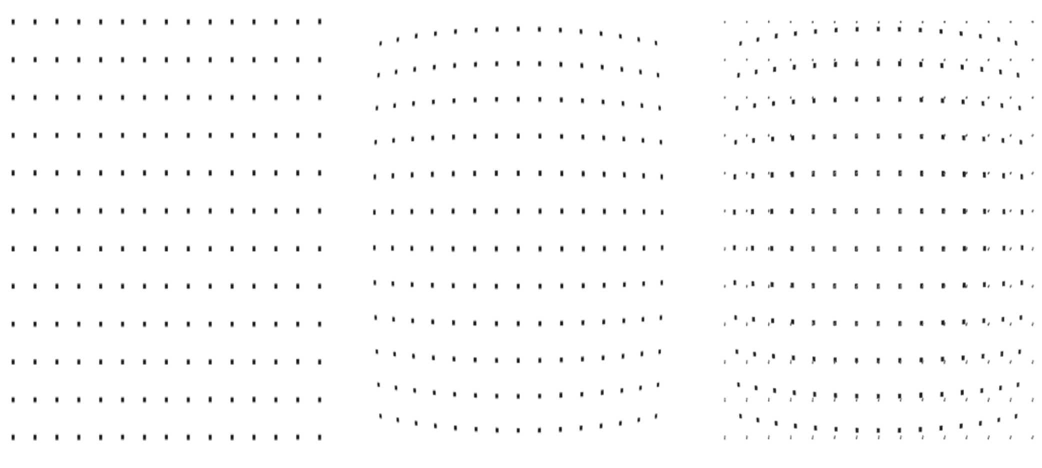

(D) Regular Undistorted Image	(E) Distorted Image	(F) Corrected Image using DMAM

Elected distortion polynomial for Lena image:	$\mathcal{F}(r) = +1.0000r^1 + 0.0000r^2 - 0.1500r^3 + 0.0000r^4 - 0.2500r^5 + 0.0000r^6 + 0.0000r^7$
The correction polynomial obtained using DMAM alg.:	$\mathcal{F}(r) = +1{,}0073r^1 - 0{,}1293r^2 + 0{,}4301r^3 - 0{,}8809r^4 - 0{,}3404r^5 + 1{,}0814r^6 - 0{,}4885r^7$

Key: (A) – set of referential marks created by hand; (B) – The Image from the biometric scanner; (C) – corrected image, small dots represents best poses of all marks after application of DMAM algorithm, large dots represents original poses of calibration marks in calibration image; (D) – original image of the Lena portrait [11]; (E) artificially distorted Lena image; (F) – undistorted image obtained using DMAM correction method.

Figure 2. Experimental Results. (A,B,C) the Image Obtained from the Biometric Scanner; (D,E,F) the Lena Testing Image

Hence, in order to make it possible to decide when the values of the vector $\boldsymbol{C_f}$ for primary-jDE are optimal, an objective function $fitness_1$ was defined – see **Algorithm 2**. Similarly objective function $fitness_2$ was defined for the second part of DMAM algorithm marked here as secondary-jDE, which defines level of correspondence between the pixels of the image $\boldsymbol{I_U}$ which have to be coloured and corresponding pixels in the image $\boldsymbol{I_D}$ supposing that vector $\boldsymbol{C_f}$ is known. Both the objective functions are defined as:

$$fitness_1: (\hat{x}, \hat{y}) = \underset{\boldsymbol{C_f} \in \mathbb{R}}{arg\ opt}\ \mathcal{F}_{primary-jDE}(M_C, M_R)$$
$$fitness_2: (x', y') = arg\ opt_{t_R \in \mathcal{H}_D}\ \mathcal{F}_{secondary-jDE}(t_R, P_W, C_f), P_W \in \mathcal{H}_U \quad (4)$$

$(\hat{x}, \hat{y})$ defines the best estimation of the position of the centre of mass of the mark M_F after application of the correction multinomial to corresponding pose defined by mark M_F with regard to the pose of the referential mark M_R. Expression (x', y') defines the best estimate of the position of the pixel in $\boldsymbol{I}_D$ with regards to vector $\boldsymbol{C_f}$, the colour of which will be moved to position $P_W(x, y)$ in the undistorted image. It holds true that $\boldsymbol{X_i}^{\boldsymbol{secondary-jDE}} \in \mathcal{H}_D$.

(A) Left side of the tested image	(B) Right side of the tested image	(C) Primary jDE optimizer convergence

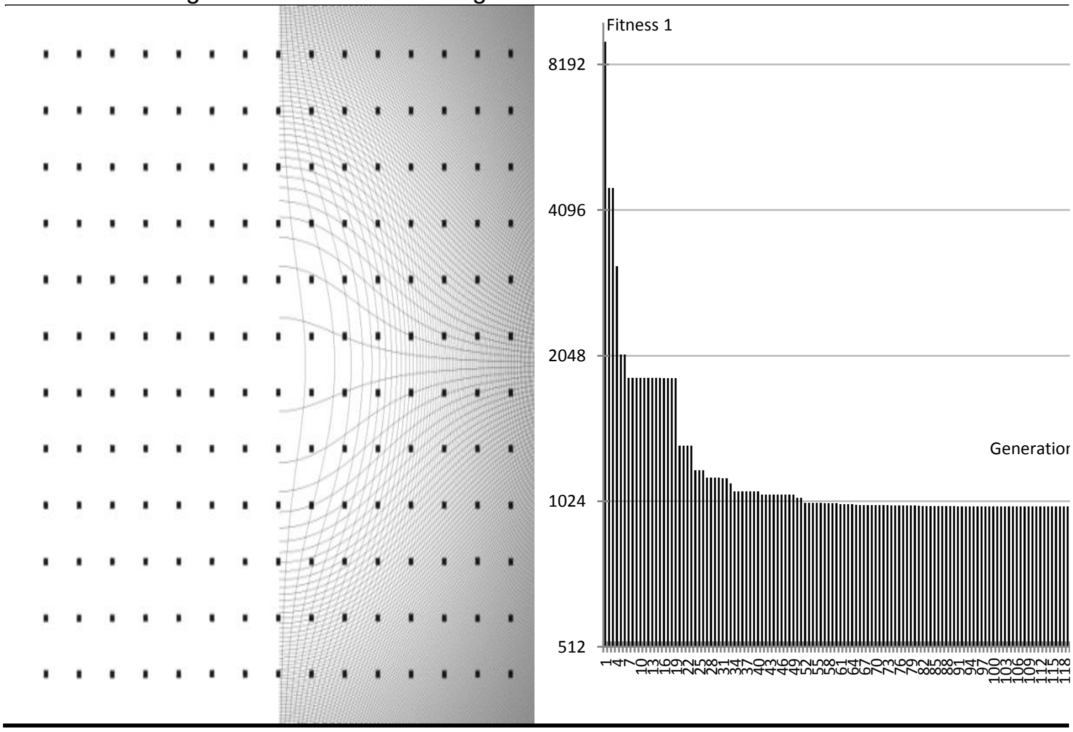

Figure 3. The Effect DMAM Filtration (A) and without DMAM Filtration Algorithm (B); (C) Result of Primary jDE Convergence

The work result of the DMAM algorithm is displayed in Figure 2A, B, C. Figure (A) depicts poses of the referential marks M_R, *i.e.*, ideal image, which must be reached. Figure (B) displays B&W image which was obtained from the biometrical scanner, and which is burdened with distortion of a small range. Figure (C) displays the final corrected image – gray dots and calibration marks are displayed as well – black dots, from image (B). Figure 3C depicts the convergence chart of $fitness_1$ function. Resulting values in single generations corresponds to the sum of Euclidean distances of the single marks M_F and M_R according to the actual coefficients $\boldsymbol{C_f}$ in pixels. The best reached value was 999.0 pixels. In regards to the manual camera adjustment, the achieved result is very good. Figure 3 depicts corrected image of calibration marks, how it looks after DMAM algorithm using and using direct-mapping method. Working parameters of the primary jDE were chosen as follows: $N = 60$, $T_1 = 120$, $\tau_1 = 0.7, \tau_2 = 0.3$, $F_u = 0.5, F_l = 0.5$, $\overline{\boldsymbol{V_p}} \equiv RandToBest/1/bin = X1 + F(Xb - X2) + F(X3 - X4)$. Vector $\overline{\boldsymbol{V_p}}$ was selected purely based on practical experiments and provided the best results. Working parameters of the secondary jDE were: $N = 20$, $T_2 = 40$, $\tau_1 = 0.7, \tau_2 = 0.3$, $F_u = 0.5, F_l = 0.5$, Vector $\overline{\boldsymbol{V_p}}$was identical to primary jDE. Accuracy and especially algorithm speed can be selected using parameters N , T_1, T_2 . Used processor was Athlon3500+/Orleans 2.2GHz. The necessary time demands were 58 minutes.

Figure 2 D, E, F shows the result of the second experiment which uses well known bitmap figure - Lena [11]. The bitmap image was first artificially distorted using multinomial $\mathcal{F}$ - see Figure 2. With use of the DMAM algorithm vector $\boldsymbol{C_f}$ - vector of correction coefficients - was then obtained. Using correction the image coefficients was corrected and reconstruction of missing pixels was performed. The final result is depicted in Figure 2E and also multinomial used for image distortion and multinomial obtained by DMAM algorithm are depicted. All working parameters were identical to the previous experiment. Resulting image – see Figure 2F is perfect and without any missing un-coloured pixels as it can be seen in Figure 3B.

3. Conclusion

This paper proposed a method of calibrated camera parameters optimization based on an advanced Differential evolution algorithm called jDE. The method uses correction polynomial of degree up to 7. The number and combinations of the used degrees can be selected manually. All experiments use full number of degrees 7. The proposed correction algorithm provides a stable and accurate method to correct barrel or pillow distortion. An advantage of proposed method DMAM is that obtained correction coefficients and position of the missing pixels are unchanging providing that the focal distance of used camera is fixed. The presented method was designed to correct an image obtained from biometrical scan of a human hand, but it can be used for any distortion correction in general.

Acknowledgment

This paper was created with a support of Ministry of Interior of the Czech Republic, grant No. VF20112015018 with the title"Citizens security - crisis management BOKR".

References

[1] A. E. Conrady, "Decentred lens-systems", Monthly Notices of the Royal Astronomical Society, vol. 79, **(1919)**, pp. 384-390.
[2] A. A. Magill, "Variation in distortion with magnification", Journal of Research of the National Bureau of Standards, vol. 54, no. 3, **(1955)**, pp. 135–142.
[3] D. C. Brown, "The simultaneous determination of the orientation and lens distortion of a photogrammetric camera", Air Force Missle Test Center - Report, Patrick AFB, Florida, vol. 50, no. 20, **(1956)**, p. 23.
[4] D. C. Brown, "Close range camera calibration", Symposium on close range photogrammetry, DBA Systems Inc., **(1971)**.
[5] J. Brest, S. Greiner, B. Bošković, M. Mernikand V. Žumer, "Self-adapting control parameters in differential evolution: A comparative study on numerical benchmark problems", IEEE Transactions on Evolutionary Computation, vol. 10, no. 6, **(2006)**, pp. 646-657.
[6] C. Liu, Y. Jia, W. Cai, T. Wang, Y. Song, X. Sunand J. Zhang, "Camera calibration optimization technique based on genetic algorithms", Journal of Chemical and Pharmaceutical Research, vol. 6, no. 1, **(2014)**, pp. 97-103.
[7] W. Kimand C. Kim, "An efficient correction method of wide-angle lens distortion for surveillance systems", IEEE International Symposium on Circuits and Systems, **(2009)**.
[8] R. Cucchiara, C. Grana, A. Pratiand R. Vezzani, "A Hough Transform-based method for Radial Lens Distortion Correction Proceedings", 12th International Conference on Image Analysis and Processing, **(2003)**.
[9] W. T. Welford, "Aberrations of Optical Systems", CRC Press, **(1986)**, p. 284.
[10] R. Stornand K. Price, "Differential evolution—A simple and efficient heuristic for global optimization over continuous spaces", Journal of Global Optimization, vol. 11, **(1997)**, pp. 341-359.
[11] http://www.ee.cityu.edu.hk/~lmpo/lenna/Lenna97.html, **(2015)**.

Authors

Jaroslav Moravec, he received the B.Sc. in informatics and the M.Sc. in theoretical and applied cybernetics, both from West Bohemia University, Faculty of Applied Sciences, Czech Republic.His research interests are in the areas of evolutionary computations, bioinformatics and computational intelligence.

Miloslav Hub, he graduated from Jan Perner Transport Faculty of University of Pardubice (the Czech Republic) at 2002. Ph.D. in 2005. Since 2004 a senior lecturer, habilitate assoc. prof. 2012 University of Pardubice. Department of System Engineering and Informatics, Faculty of Economics and Public Administration, University of Pardubice. He deals with software engineering, usability engineering and data security and he is a member of Usability Professional Association and Association for Computing Machinery.